Electrical Parameters Characterization of Aged IGBTs by Thermo-Electrical Overstress

Evan Dimech

The Department of Electronic Engineering
The University of York
Heslington, York, UK

John Frederick Dawson

The Department of Electronic Engineering
The University of York
Heslington, York, UK

Abstract — **During their lifetime, power semiconductor devices such as Insulated Gate Bipolar Transistors (IGBTs) can suffer from different failure mechanisms. This paper reports the monitored changes in the electrical parameters of tested IGBTs when subjected to accelerated ageing through thermo-electrical overstress. The changes are indicative that the device is at the onset of failure and hence can be utilized within prognostic techniques so as to determine the health state of the device. The study describes how the accelerated ageing strategy was implemented providing details of the implemented hardware and software. Tested IGBTs were characterized before, during and after accelerated ageing. Details of the IGBT characterization setup are provided. Furthermore, the corresponding monitored changes in the die-attach X-Ray imagery, gate threshold voltage, collector leakage current, transfer characteristics, transconductance, output characteristics and internal free-wheeling diode forward characteristics are presented and discussed.**

Keywords—insulated gate bipolar transistors, accelerated ageing, electrical parameters characterization, precurssors, prognostics

I. Introduction

Today power-electronic converters, drives and modern electric machines play a very important role in the performance and overall operation of ships, aircraft, space crafts, ground vehicles, and industrial applications. Such power-electronic systems utilize power semiconductor devices for power load activation and control. Failure of these devices can limit system operation or may lead to failure, which within the applications mentioned, can be mission critical, safety-critical or even life-threatening. During their lifetime, power semiconductor devices such as Insulated Gate Bipolar Transistors (IGBTs) can be affected by many failure mechanisms such as electro migration, gate oxide degradation, dielectric breakdown, thermal instability or hot carrier injection. This paper describes the monitored changes in the electrical parameters of tested IGBTs when subjected to accelerated ageing. The changes are indicative that the device is at the onset of failure and hence can be utilized within prognostic techniques so as to determine the health state of the device. The IGBT structure combines the physics of a power MOSFET and power bipolar junction transistor (BJT) integrated in the same die hence offering the gated input of the power MOSFET and the output capabilities of a power BJT. Fig. 1 illustrates the IGBT cell structure, utilized during this study, which is constructed similarly to a vertical diffused power MOSFET. The main difference is the inclusion of the P+ collector layer. This modification forms a vertical PNP BJT. The additional P+ region will form, the cascaded connection of the surface power MOSFET and the underlying BJT. This P+ region forms a PN junction with the N- drift region. Conduction modulation occurs by injecting minority carriers in the drift region. This leads to a larger current density than the power MOSFET, while the forward voltage drop is reduced [1]. Once the IGBT is switched off, the excess carriers in the N- drift region decay by electron-hole recombination, which causes a gradual collector current decay. Similar to other minority carrier devices there is a compromise between the on-state losses and faster switching speeds. The four-layer NPNP structure of the IGBT has a parasitic thyristor. Turn-on of this thyristor is undesirable, as it will lead to the loss of control by the gate. Ideally, once minority carriers are injected into the drift region, they should flow to the emitter region directly. The electrons charge in the formed MOSFET n-channel attracts the majority of holes. This attraction causes a lateral "holes current" through the p-type region. This current flow flowing through the p-type region develops a corresponding voltage drop across the p-type region spreading resistance. If this voltage drop is large enough, it can forward bias the base-emitter junction of the parasitic NPN transistor. This will trigger the parasitic thyristor structure, latching up the IGBT, thus losing gate control.
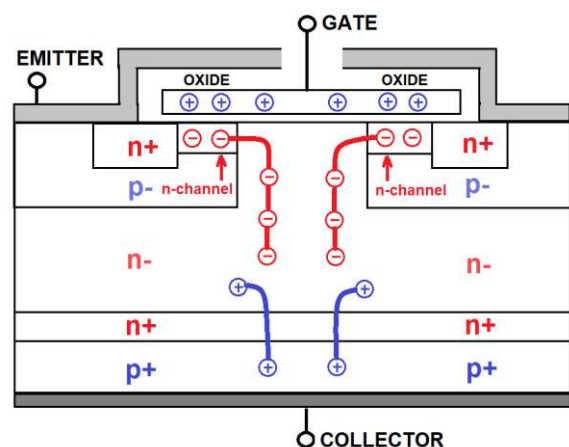

Fig. 1. IGBT Cell Structure

II. IGBT Accelerated Ageing

A. Developed Accelerated Ageing System Hardware

The accelerated ageing system developed is intended to accommodate commercially available gated-power transistors. The ageing technique is based on the one developed by Sonnenfield et al [4], utilizing a thermo-electric overstress approach, where the device will experience power pulses without the use of a heat sink so as to cause self-heating. The system was designed to autonomously monitor and control the device temperature while recording electrical and environmental parameters. Fig. 2 illustrates the architecture of the system, consisting of; commercial instrumentation, with custom built hardware and software.
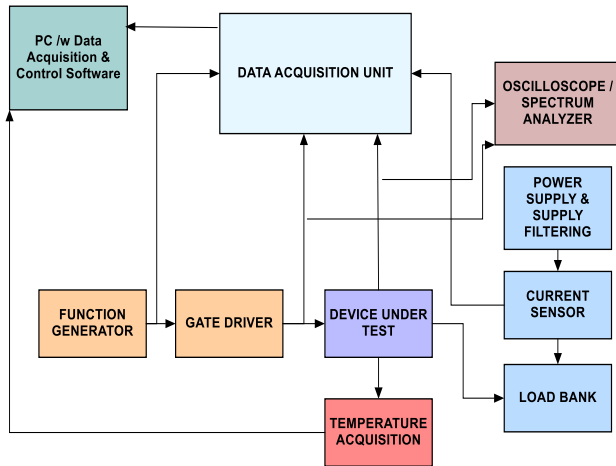

Fig. 2. Overview of the Accelerated Ageing System Architecture

The commercial instrumentation includes a Tektronix MDO4104B-3 Mixed Domain Oscilloscope; a Tektronix AFG3051C programmable function generator; for generating gate signals, National Instruments NI-9211 4-channel thermocouple module for temperature acquisition; and a NI-USB-6341 which is a multi-function data acquisition device (DAQ). The DAQ was utilized for the acquisition of the device's electrical signals during ageing; and to control the thermal ageing process. Three different power supplies were utilized. A DELTA SM 70-45 D which is a 70V, 45A power supply, solely utilized as the power source for the power pulses through the Device Under Test (DUT). Two other DC power supplies, were used for powering the signal conditioning and acquisition electronics within the custom-built hardware.

Fig. 3 illustrates the printed circuit board (PCB) for IGBT accelerated ageing. The DUT circuit is operated in a common-emitter/source configuration. The circuit consists of an IXYS IXDD614 high-speed gate driver with a 14A sink/source capability for driving the large input capacitance of the DUT. Furthermore, it is capable of operating with a maximum input voltage of 35V hence exceeding the typical 20V transistor gate limit if gate overstress is required. It can produce rise times and fall times less than 30ns. It also has an integrated "Enable"

functionality that isolates the gate driver output from the gate of the transistor. This is used by the temperature controller to control the transistor case temperature. On the output side of the transistor, an LTS-6NP Hall-effect current transducer capable of measuring DC, AC and pulsed currents up to 40A with a frequency bandwidth up to 100kHz is used.

Fig. 3. Accelerated Ageing System Custom Built PCB

A protection relay was utilized in series with the load to switch the DUT's power, off in case it goes into latch-up, hence avoiding thermal runaway, and device destruction. Three large capacitors were connected in parallel with the DUT's power supply to filter cable inductance effects and power supply interference. Node voltages including the gate voltage V_G, emitter/source V_E, collector/drain voltage V_C, gate driver output $V_{DRIVE,}$ function generator output V_{GEN}, transduced collector/drain current I_C, were all buffered, over and under voltage protected, and fed via BNC connectors to the NI-DAQ analogue inputs. BNC connectors were added at important nodes such as the gate, emitter/source, and collector/drain to provide a direct connection for oscilloscope inputs to acquire switching waveforms during the ageing process. The circuit was implemented on a four-layer PCB with dedicated power bus, ground, analogue signal, and power section layers.

B. Developed Accelerated Ageing System Software

Software was developed within National Instruments (NI) Labview environment to control the ageing process and acquire and log electrical and thermal parameters during ageing. The software maintains the DUT's case temperature to the value specified by the Temperature Control Set Point parameter within a specified Hysteresis Band. This is achieved by enabling the gate driver output hence pulsing the device to cause self-heating. When the upper temperature value of the hysteresis band is reached the gate driver output is disabled, leaving the device to cool, until the lower temperature of the hysteresis band is reached, when the gate driver output is enabled again. This procedure continues until the DUT latches-up. When the DUT's temperature reaches the set Thermal Runaway temperature value, the power relay is de-energized, avoiding the destruction of the device. At this point the device is left to cool down to 25^0C, ending an ageing iteration cycle. This cycle is repeated at least three times for each device, for a full ageing procedure to be completed.
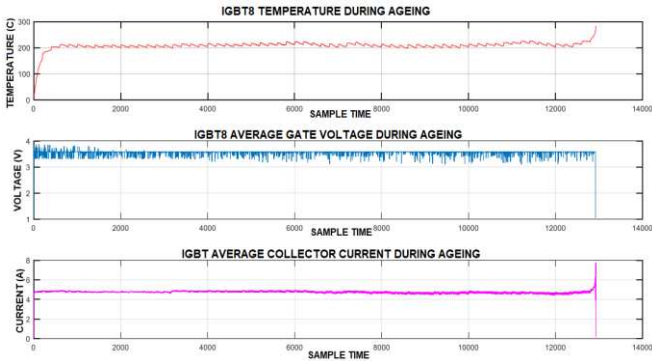
Fig. 4. IGBT8 Age Iteration highlighting DUT latch-up and corresponding thermal runaway.

C. IGBT Accelerated Ageing Setup Procedure & Details

Accelerated ageing was conducted on the International Rectifier IRG4BC30KDPBF TO-220 600V/16A IGBT [9]. The accelerated ageing test conditions were set with an output stage supply voltage of 7V DC; two series 0.25Ω 1% 25W resistors as load; and a gate input signal of 12V at 10kHz with a 50% duty cycle. A type K thermocouple was attached to the DUT by drilling a 1.1mm hole in the epoxy cover on the front side. After some experimentation, a jig was built to penetrate the same depth at the same position within the epoxy without touching critical parts of the DUT. The thermocouple has a tight fit (thermocouple width of 1mm) with the DUT. The temperature control set point was set to 270˚C, with a hysteresis band of +/-3˚C and a thermal runaway limit of 285˚C. These settings proved to trigger latch-ups within minutes. It was noticed that for a new IGBT, the device will latch-up and fail quite quickly. With each ageing iteration, it will tend to take longer until latch-up failure occurs. Moreover, as discussed later on, it is the first ageing iteration which triggers the largest characteristic change in the device. Failure manifests itself as an increase in the collector current (I_C) throughout an age iteration. This is mainly due the negative temperature coefficient of V_{CE_SAT} for (for $I_C < 10A$) [9]. IGBTs being a minority carrier device suffer from "residual current" during turn-off. It was noticed that during the ageing procedure this "residual current" increases in magnitude. There will come a point where the "residual current" is large enough to cause the on-set of the DUT's latch-up. At that point the collector current increases abruptly leading to thermal runaway. Fig. 4 shows the DUT temperature, gate voltage, and collector current during an age iteration procedure for IGBT8. The final stage of each plot highlights the loss of gate control, abrupt increase of the collector current and the corresponding thermal runaway. All of the aged devices presented in this study remained functional (switching appropriately) after the three ageing iterations. This demonstrates that the process is only degrading not destroying the devices. Further to the electrical and thermal characterization parameters acquired during ageing, two source meter units (SMUs) in conjunction with custom-built software and hardware were utilized to measure the DUT electrical parameters when new and after each age iteration.

The SMUs utilized were, the Keithley 2400 four-quadrant SMU and the Keithley 2461 four-quadrant power SMU with a pulsed capability of 10A 100V and with voltage and current measurement resolution of 5µV and 50pA respectively. The SMUs 2400 and 2461were interfaced with the PC via RS232 and USB respectively. A Test-Switching PCB was designed and developed to automatically configure the DUT for the different characterization tests. A thermoelectric cooler (Peltier Element) in conjunction with a controller was used to control the DUT temperature to 25˚C. This ensures that the electrical characterization measurements are isolated from any temperature changes. During characterization, current and voltage pulses with low pulse duration and duty cycle were utilized so as to ensure that the DUT does not self-heat during the test. As high current testing produces voltage drops along the leads, a four Wire/Kelvin measurement technique was used.

III. IGBT AGEING CHARACTERIZATION RESULTS

A. X-Ray Analysis

X-Ray analysis was conducted so as to determine effects produced by the ageing strategy on the IGBT mechanical package. This was undertaken using the NORDSON DAGE Jade X-Ray machine. Fig. 5 shows X-Ray analysis of IGBT6 from new to after three age iterations. The imagery illustrates the IGBT "co-pack" package with an integrated free-wheeling diode on the right and IGBT structure on the left (large area). These two areas characterize the die-attach of both devices. Silicon (Si) is invisible to X-Rays and hence reflections are produced by the die-attach layer. The die-attach layer has two main purposes: mechanical adhesion of the die to the substrate and dissipation of heat generated in the die [6]. In power devices heat densities are high, so conventional die-attach adhesives or eutectic solder alloys are not suitable. In this case high-melting solder alloys are used. Die-attach materials are required to dissipate high heat throughout the device's lifetime. Hence the solder alloy must cover completely the surface between the lead-frame and die with a low void rate on the die attach layer. Typically, for high power applications, the maximum void rate permitted is 5% [6].
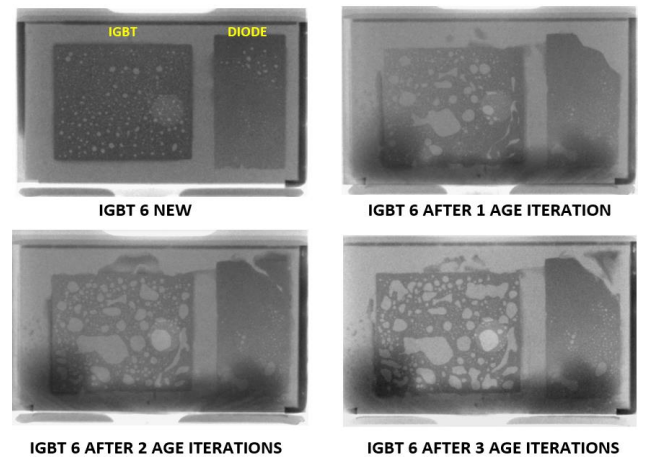

Fig. 5. X-Ray analysis progression of IGBT6 after three age iterations.

As illustrated in Fig. 5 the dark areas within the two structures indicate good die-attach adhesion, while the bright areas indicate voids. It is evident that, with each age iteration, there is an increase in the amount and severity of voids within the two die-attaches. All aged IGBTs have an increase in die-attach voiding and melting, even though there were variations. This is highlighted when comparing X-Ray image for IGBT6 and IGBT8. Fig. 7 illustrates the resultant X-Ray imagery for IGBT17 which was exposed to eight age iterations finally leading to a permanently damaged short-circuited output. One can appreciate the severity of die-attach voiding and erosion.
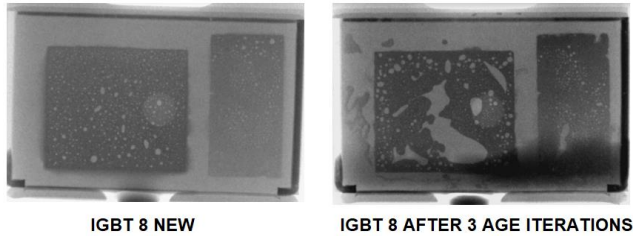

IGBT 8 NEW **IGBT 8 AFTER 3 AGE ITERATIONS**

Fig. 6.   X-Ray analysis of IGBT8 new and after three age iterations

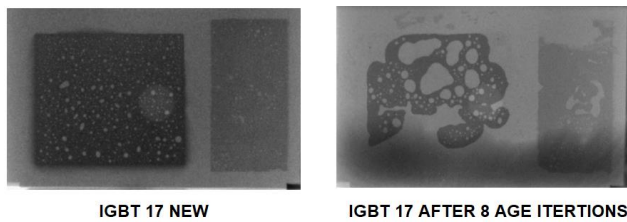**IGBT 17 NEW** **IGBT 17 AFTER 8 AGE ITERTIONS**

Fig. 7.   X-Ray analysis of IGBT8 new and after eight age iterations which led to device destruction.

B. IGBT Threshold Voltage & Leakage Current

The IGBT's threshold voltage is the minimum gate-to-emitter voltage (V_{GE}) needed to create a current of 250µA between the collector and emitter at 25˚C. It was observed that all of the tested IGBTs exhibited an increase in the threshold voltage with every age iteration. This is illustrated in Fig. 8.
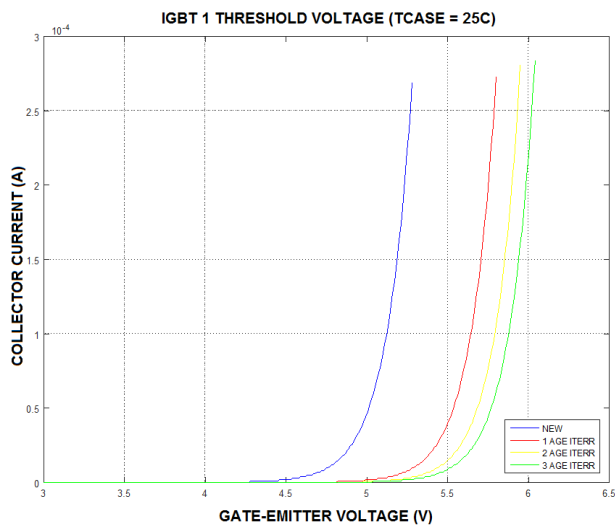

Fig. 8.   IGBT1 gate threshold voltage variation with age iterations.

After three age iterations, the average threshold voltage increase was 12.1%, with the maximum increase was of 14.2% for IGBT1 and IGBT8. This is illustrated in Fig. 9. The increase in threshold voltage is an indicator of gate dielectric oxide degradation [6]. In relation to the collector leakage current, all of the tested IGBTs remained with leakage currents below 1µA before and after accelerated ageing. It is important to mention that all of the tested IGBTs survived ageing.
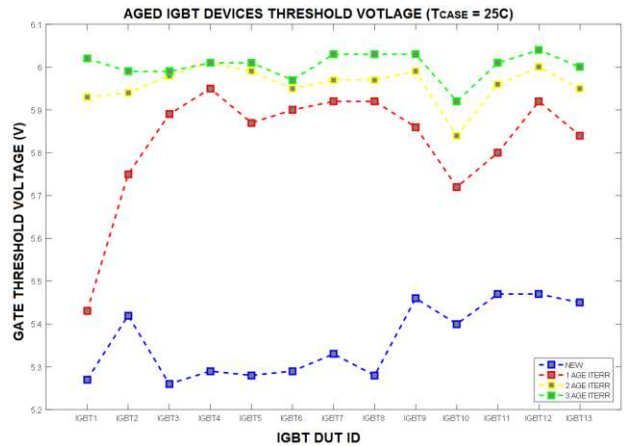

Fig. 9.   Tested IGBTs gate threshold voltage variation with ageing.

C. IGBT On-State Voltage (V_{CE_ON}) / On-State Resistance & Output Characteristics

The tested IGBT collector-emitter on-state voltage (V_{CE_ON}), is temperature dependent, with negative temperature coefficient (for I_C < 10A) [9]. Fig. 10 shows the negative temperature coefficient of V_{CE_ON} for IGBT3. It was noticed that this negative temperature relationship becomes less evident with subsequent age iterations.
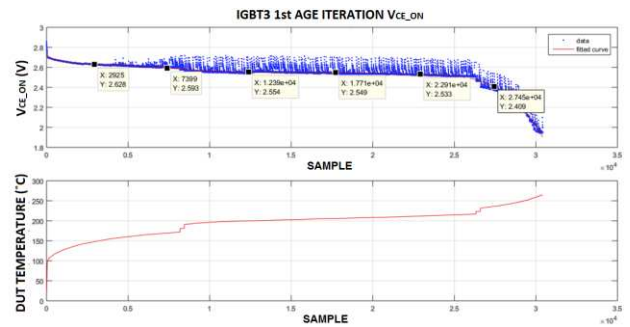

Fig. 10.   VCE_ON variation during 1st ageing iteration of IGBT3.

Furthermore, the initial V_{CE_ON} decreased with each age iteration. In the case of IGBT3, it decreased from around 2.8V when the device was new to around 2.4V at the beginning of the third age iteration. This indicates that V_{CE_ON} had a permanent change due to device ageing. V_{CE_ON} was characterized at the beginning when the device was new and after each ageing iteration, at a device temperature of 25˚C. Measurement was conducted by providing a 7A current pulse through the collector at a gate voltage (V_G) of 15V, measuring the corresponding collector to emitter voltage pulse (V_{CE}).

From the results obtained, one can observe a decrease in the effective on-state resistance for all tested IGBTs. Since the collector current pulse amplitude was constant (7A), this directly indicates that it is effectively the on-state voltage V_{CE_ON} which has decreased. After three age iterations, the average effective on-state resistance percentage decrease over that of a new device, was of 22.3% with a maximum percentage decrease of 27.7% for IGBT5.
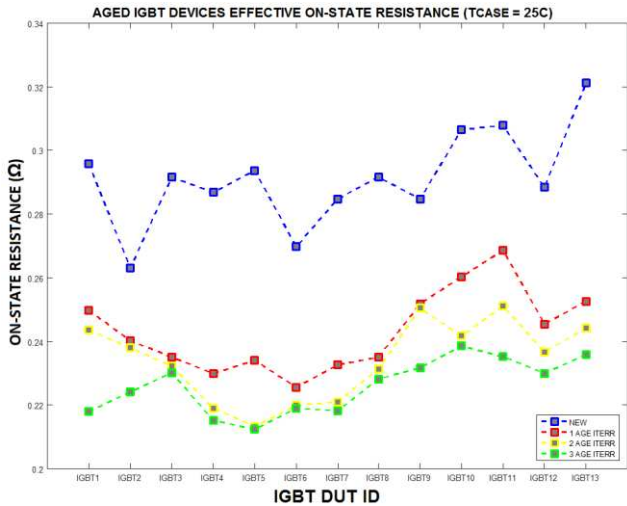

Fig. 11.   Tested IGBTs effective on-state resistance variation with ageing.

Furthermore, the output characteristics of every tested IGBT were determined before and after each age iteration, at a case temperature of 25˚C. Fig. 12 shows the output characteristics variation of IGBT10 for the first 7A of collector current (I_C) hence the linear part of the output characteristics. One can observe that for the same value of collector-emitter voltage (V_{CE}), the corresponding collector current (I_C) has increased with each age iteration. This indicates that the effective resistance of the device has decreased. It is important to highlight the fact that each tested IGBT exhibited similar changes in their respective output characteristics.
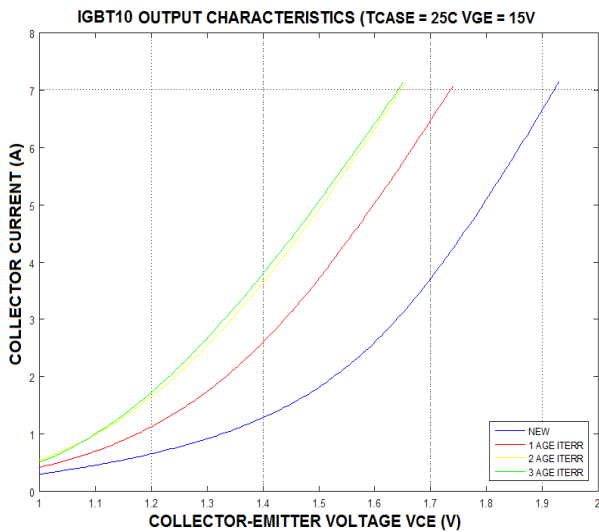

Fig. 12.   IGBT10 output characteristics variation with ageing.

D. IGBT Transfer Characteristics & Transconductance (g_{fe})

The transfer characteristics were determined for every tested IGBT before and after each age iteration, at a device's case temperature of 25˚C. Fig. 13 shows the transfer characteristics of IGBT11, for the first 7A of collector current (I_C). One can observe that for the same gate-to-emitter voltage (V_{GE}) the corresponding collector current has decreased with each age iteration. All of the other tested IGBTs experienced similar changes in the transfer characteristics. This indicates a decrease in the forward transconductance (g_{fe}) of the device.
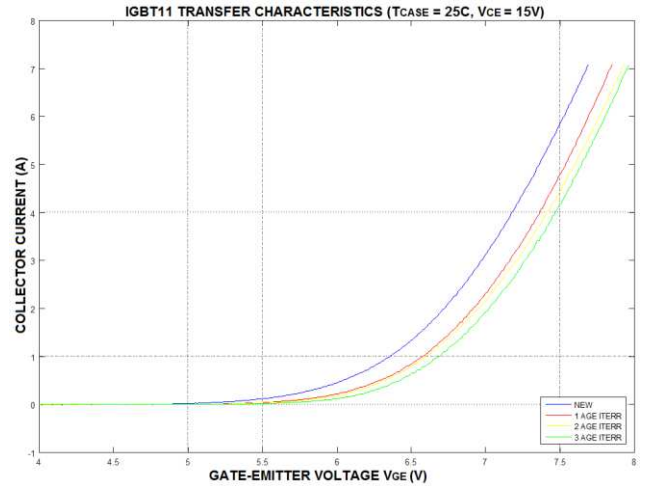

Fig. 13.   IGBT11 transfer characteristics variation with ageing

The forward transconductance was determined by calculating the slope of the linear region of the transfer characteristics. In Fig. 14 one can observe that each tested IGBT experienced a decrease in the forward transconductance with every age iteration. This result is in accordance with the observed gate threshold voltage increase with ageing, which is inversely related with the forward transconductance.   After three age iterations, the average forward transconductance percentage decrease over that of a new device, was of 15% with a maximum percentage decrease of 18.25% for IGBT3.
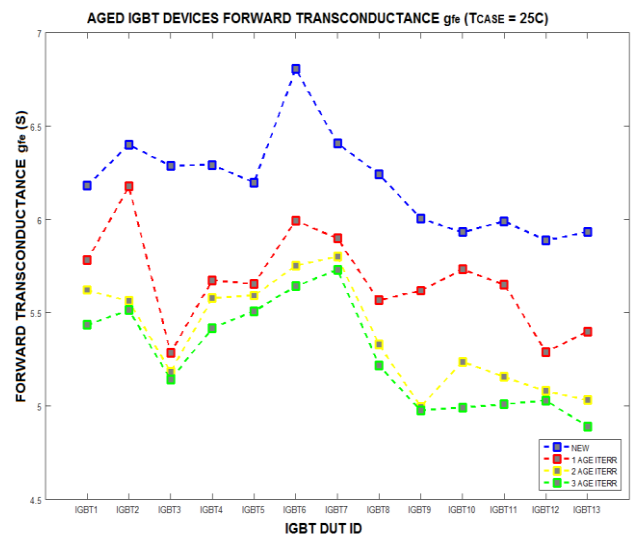

Fig. 14.   Tested IGBTs forward transconductance variation with ageing

E. IGBT Internal Diode Forward Voltage Drop (V_FM)

The internal diode forward voltage characteristics were determined for every tested IGBT, before and after ageing. The devices' temperature was set to 25˚C during measurement. Fig. 15 shows the internal diode, forward characteristics of IGBT3, up to 7A forward current (I_F). One can observe that for the same forward current, the corresponding internal diode's forward voltage (V_{FM}) has decreased. All of the other tested IGBTs experienced similar changes in their internal diode's forward characteristics.
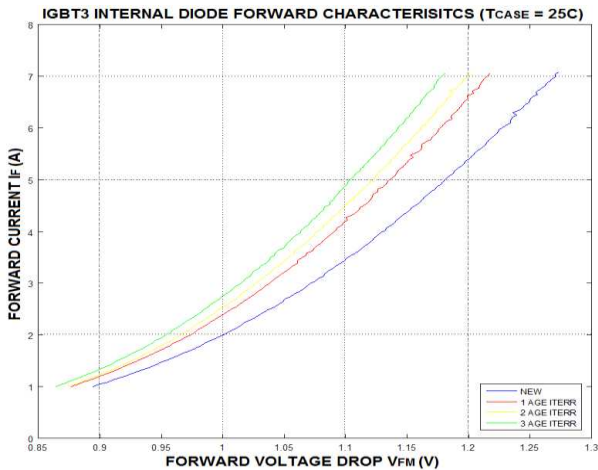

Fig. 15.   IGBT3 diode's forward characteristics variation with ageing.

In Fig.16 one can observe that each tested IGBT experienced a decrease in the diode's forward voltage with every age iteration. After three age iterations, the average diode's forward voltage percentage decrease was of 5.5% with a maximum percentage decrease of 9.9% for IGBT4.
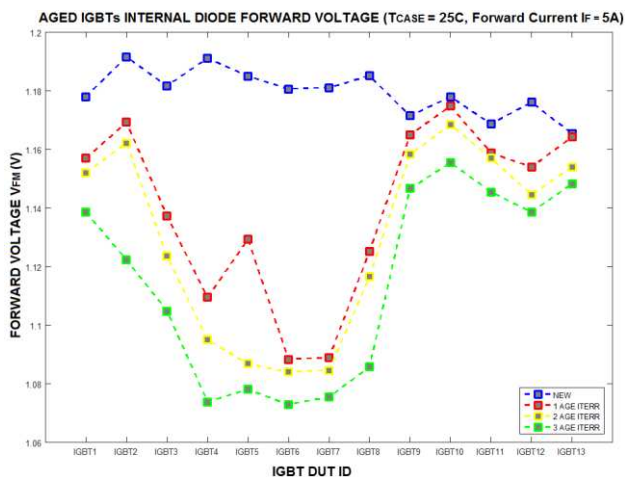

Fig. 16.   Tested IGBTs Diode Forward Voltage variation with ageing.

IV.   DISCUSSION AND CONCLUSION

The characterization of aged IGBTs, shows that the implemented thermo-electric ageing strategy, produces damage mechanisms within the IGBTs' structure which consequently alters the corresponding electrical parameters.

X-Ray imagery evidenced die-attach degradation during ageing due to an increase in voiding and melting. This definitely impacted the device's output characteristics mainly a decrease in the device's on-state voltage V_{CE_ON} and hence a decrease in the effective on-state resistance. Looking at Fig. 5, corresponding to IGBT6 shows, that it was the first age iteration which produced the biggest change in voiding. The same can be said for the effective on-state resistance of IGBT6, where it was the first age iteration which produced the biggest changes, while consecutive age iterations produce changes of a lesser degree. This trend was present in all tested devices and the corresponding electrical parameters. The die-attach plays a fundamental role in the heat dissipation of the device. As suggested by Patil et al [6], the degradation of the die-attach will impact the devices' PN junction (closest to the collector) thermal impedance. This means that after ageing this junction will experience higher temperatures when compared to new. This leads to a higher concentration of charge carriers, which leads to the decrease of the effective on-state resistance. This analysis can be extended to the internal free-wheeling diode die-attach degradation, which affects the thermal impedance of the diode's PN junction, leading to a higher charge carrier concentration This explains why the internal diode's forward voltage drop decreased after ageing. Furthermore, the utilized ageing strategy produced a gate dielectric degradation. This is evidenced by the increase in the gate threshold voltage and decrease in the forward transconductance, due to trapped electrons within the gate oxide [6]. Current and future extensions of this work will include the characterization of the IGBT's switching parameters, in relation to IGBT ageing.

REFERENCES

[1]   M.H. Rashid, *Power Electronics Handbook, Devices, Circuits & Applications*, 3rd Edition, Oxford, UK, BH-Elsevier, 2011

[2]   Baliga, B. Jayant. "*Fundamentals of Power Semiconductor Devices*". *Boston*: New York, Springer, 2008.

[3]   B. Saha, J. R. Celaya, P. F. Wysocki, and K. F. Goebel, "Towards prognostics for electronics components," in IEEE Aerospace conference, 2009, pp. 1-7.

[4]   G. Sonnenfeld, K. Goebel, and J. R. Celaya, "An agile accelerated aging, characterization and scenario simulation system for gate controlled power transistors," in IEEEAUTOTESTCON, 2008

[5]   A. Ginart, M. Roemer, P. Kalgren, and K. Goebel, "Modeling Aging Effects of IGBTs in Power Drives by Ringing Characterization," in IEEE International Conference on Prognostics and Health Management, 2008.

[6]   N. Patil, J. Celaya, D. Das, K. Goebel, and M. Pecht, "Precursor Parameter Identification for Insulated Gate Bipolar Transistor (IGBT) Prognostics," IEEE Transactions on Reliability vol. 58, pp. 271-276, 2009.

[7]   J. R. Celaya, N. Patil, S. Saha, P. Wysocki, and K. Goebel, "Towards Accelerated Aging Methodologies and Health Management of Power MOSFETs (Technical Brief)," in Annual Conference of the Prognostics and Health Management Society 2009, San Diego, CA., 2009

[8]   J. R. Celaya, N. Patil, S. Saha, P. Wysocki, V Vashcenko, "Accelerated Aging System for Prognostics of Power Semiconductors" AUTOTESTCON, 2010 IEEE, Orlando, USA, 2010.

[9]   "International rectifier IRG4BC30KDPbF datasheet," [Online]. Last Accessed: 15/04/2018.